A Framework for 3D Reconstruction of Concrete Box-Girder Interiors from Point Cloud Data

Taegyu Kim[a], Seunghun Im[a], Duho Chung[a], Sungwoo Cho[a], Ilhyoung Shin[b], Hyeongu Ji[b] and Hyoungkwan Kim[a*]

[a]Department of Civil and Environmental Engineering, Yonsei University, Korea
E-mail tacoskywalker@yonsei.ac.kr, imseunghun4006@yonsei.ac.kr, jungduho1@yonsei.ac.kr, paul0524@yonsei.ac.kr and hyoungkwan@yonsei.ac.kr
[b]Dangjin Branch, Korea Expressway Corporation, Korea
E-mail niceguy@ex.co.kr and jeehw@ex.co.kr

Abstract –

Inspection of concrete box-girders is essential for ensuring the structural performance of a PSM bridge throughout its service life. With advances in 3D sensing and point cloud processing, 3D data-based approaches have been increasingly applied to bridge inspection. This paper presents a 3D reconstruction pipeline for concrete box-girder interiors that generates CAD models directly from scan data. Point cloud data of girder interiors acquired by a quadruped robot equipped with a LiDAR sensor are preprocessed and then semantically segmented into interior components using a deep learning model. Segmented point cloud data is subsequently converted into a 3D CAD model through a sliced patch-based reconstruction algorithm. The proposed method was validated on real concrete box-girder interior data. Point cloud segmentation achieved a mIoU of 94.1%. The geometric accuracy of the generated CAD models was evaluated using mesh-to-point cloud distance, yielding mean distances of 0.025 m against point cloud data. These results demonstrate that the proposed pipeline can effectively construct as-built 3D models of concrete box-girder interiors, supporting efficient data-driven inspection.

Keywords –

Concrete Box-Girder; Point Cloud Data; Deep Learning; 3D Semantic Segmentation; 3D CAD Modeling; Robotic Data Acquisition.

1 Introduction

Bridge inspection is essential for ensuring structural performance throughout the entire service life. In particular, the internal inspection of bridges constructed using the Precast Segmental Method (PSM) has become an issue of growing concern. In 2016, corrosion and rupture of tendons were observed inside the concrete box-girder of Jeongneungcheon Overpass [1], and in 2020, tendon corrosion was identified at Cheongdam 1st Bridge [2]. Such cases of inadequate internal inspection have shown the critical importance of interior inspection for concrete box-girders.

Recent advances in 3D sensing technologies and point cloud processing have highlighted the potential of Scan-to-BIM and digital twin approaches for improving bridge inspection [3]. Jing et al. [4] proposed a method for semantic segmentation of masonry bridge components using a segmentation model trained solely on synthetic data, followed by instance segmentation using the DBSCAN algorithm. Kim et al. [5] applied SuperPoint Transformer to segment bridge point cloud data acquired by UAV-mounted LiDAR, training the model on both synthetic and real data. Yang et al. [6] presented a Scan-to-BIM framework for highway bridges, in which a deep-learning segmentation model trained on both synthetic and real datasets segments LiDAR-acquired point clouds into individual components, and the resulting segmented point clouds are then projected to extract component outlines that are subsequently parameterized and instantiated as BIM elements. Shu et al. [7] proposed an automated method to generate geometric digital twins of box-girder bridges, using a model trained on synthetic and TLS point clouds for component segmentation and cross-section key point extraction, and aligning internal structures generated from design drawings to the global coordinate system. Zhu et al. [8] proposed a method for cable-supported bridges with girders that uses TLS to scan the girder interior and processes interior and exterior point clouds to estimate the girder volume, including the internal void geometry.

Existing research have primarily focused on reconstructing external geometry or have relied on design drawings to model internal structures. Despite the importance of concrete box-girders, research on 3D data-driven inspection of box-girder interiors remains limited.

This highlights the need for methodologies to construct as-built 3D models specifically for concrete box-girder interiors.

This paper proposes a 3D reconstruction pipeline for concrete box-girder interiors based on point cloud semantic segmentation and a sliced patch-based 3D reconstruction algorithm. The proposed pipeline semantically segments structural components from interior scan data and reconstructs them into 3D models. Figure 1 illustrates an overview of the proposed pipeline. First, interior point cloud data are obtained from raw scans acquired by a LiDAR sensor mounted on a quadruped robot. Second, wall surfaces are extracted and reconstructed as parametric models to define the interior geometry. Third, the remaining interior components are semantically segmented using a deep learning-based segmentation model. Fourth, 3D CAD models of the segmented components are generated through a sliced patch-based algorithm.

2 Methodology

2.1 Point Cloud Data Acquisition and Preprocessing

As shown in Figure 1(a), interior data were acquired using a quadruped robot (Unitree Go2) equipped with a LiDAR sensor (Livox Avia) and a mini computer (Intel NUC). The acquired data were registered into a global map using FAST-LIO2 [9], and a loop-closure module was additionally integrated to correct accumulated drift and improve global consistency [10]. First, roll and pitch correction and axis alignment are performed to align the coordinate system such that the longitudinal direction of the girder is parallel to the X-axis. Then, the diaphragms at both ends of the girder were manually removed.

2.2 Wall Extraction and 3D CAD Model Generation

To extract wall surfaces from the preprocessed point cloud, this paper developed an alpha shape-based wall extraction algorithm. Figure 2(a) illustrates the stages of the proposed algorithm. First, the point cloud is projected

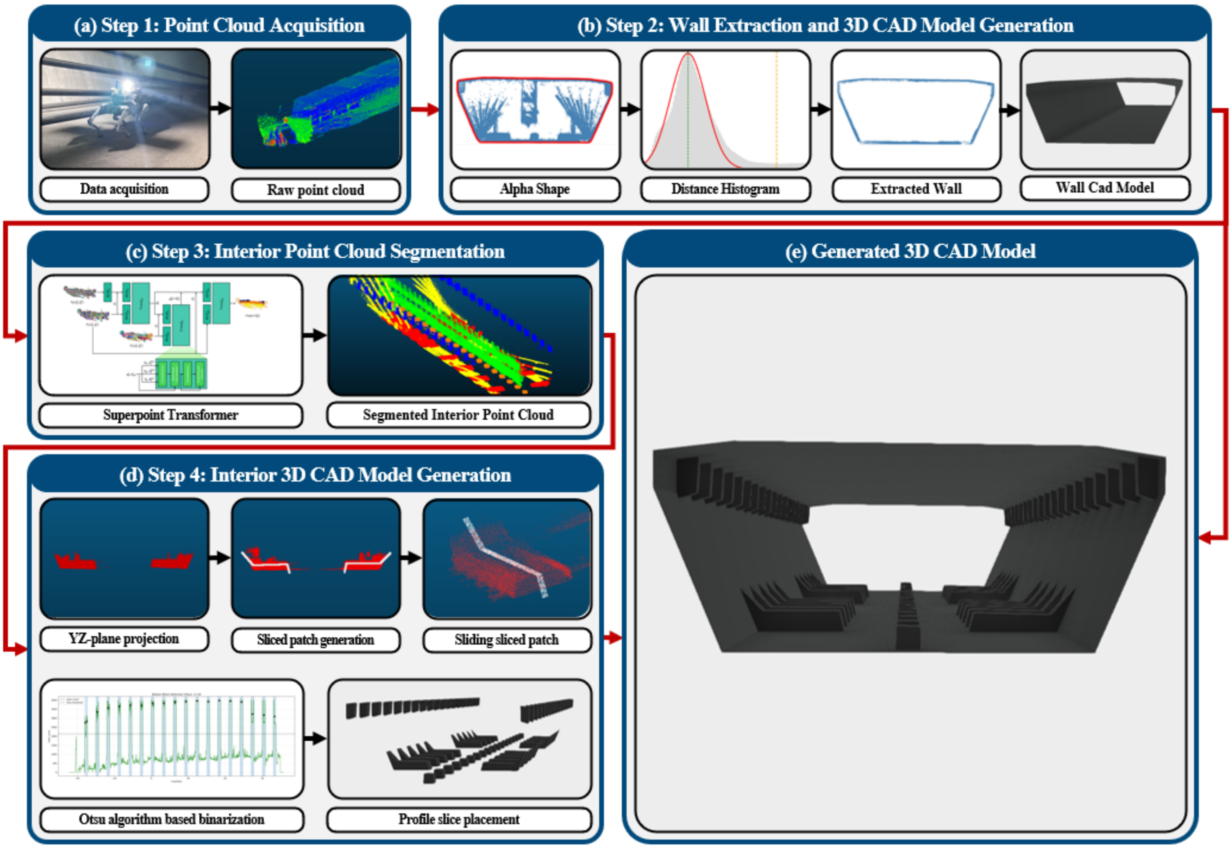

Figure 1. Overview of the proposed framework; (a) acquisition of box-girder interior point cloud data using a quadruped robot, (b) wall extraction and 3D CAD model generation, (c) point cloud segmentation using SuperPoint Transformer, (d) 3D CAD model generation of segmented components, (e) generated 3D CAD model.

onto the YZ plane, and the alpha shape algorithm is applied to estimate the outer contour of the girder cross-section. Statistical Outlier Removal (SOR) is applied prior to prevent errors caused by outliers. Second, the minimum Euclidean distance from each point in the full point cloud to the contour is computed. Third, the distribution of wall point distances is modeled as a Gaussian distribution. The peak of the distance distribution is defined as the mean μ. Since the portion of the histogram beyond the peak contains interior points, the Gaussian distribution is fitted only to the portion up to the peak. A threshold is then set at $\mu + n\sigma$ to separate wall points from interior points. In this study, a threshold of $\mu + 6\sigma$ was used, corresponding to a 99.99% inclusion probability. Finally, points within this threshold are classified as wall points, while the remaining points are classified as interior points. Figure 2(b) illustrates the generation of a 3D CAD model based on the extracted wall points. RANSAC-based line feature extraction [11] is first applied to the contour to extract parametric line segments representing the wall surfaces. The extracted line segments are then inwardly offset to μ to align them with the actual wall surface location. Finally, the cross-section is extruded along the longitudinal axis by the length of the girder to produce a parametric 3D model of the wall surfaces.

2.3 Point Cloud Segmentation

The preprocessed point cloud data is semantically segmented using SuperPoint Transformer, a deep learning-based 3D segmentation model [12]. SuperPoint Transformer (SPT) processes large-scale point clouds by first computing a multi-scale hierarchical partition of the scene into geometrically homogeneous superpoints. At each partition level, adjacent superpoints are connected to form a superpoint graph. The network then performs sparse self-attention on these graphs to propagate information at each scale, enabling large receptive fields and context aggregation while predicting semantic labels at the finest superpoint level. The interior components of the concrete box-girder are classified into five categories: deviator block, tendon, top temporary Post Tensioning (PT) bar anchor block, bottom temporary PT bar anchor block, and cable tray. A deviator block is a concrete block installed to redirect the alignment of external tendons, with embedded ducts through which tendons pass. The top and bottom temporary PT bar anchor blocks are used to apply compressive stress when joining segments during construction and are located at the top and bottom of the girder, respectively [13]. A tendon is a steel strand, and a cable tray is a metal structure that accommodates electrical and communication cables.

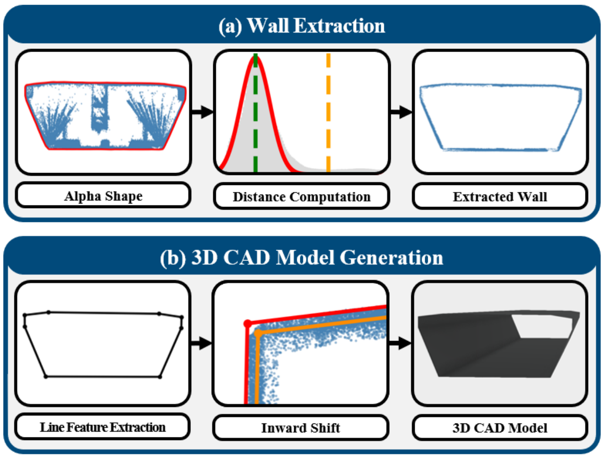

Figure 2. Extraction of the wall point cloud and 3D CAD model generation; (a) wall extraction, and (b) 3D CAD model generation.

2.4 Interior 3D CAD Model Generation

Among the five segmented classes, the deviator block, top temporary PT bar anchor block, and bottom temporary PT bar anchor block were converted into CAD models.

For 3D model generation, this paper developed a sliced patch-based 3D reconstruction algorithm. This algorithm is based on the patch-based component matching algorithm proposed by Kim et al. [14]. In their approach, a 3D patch similar in size and shape to each

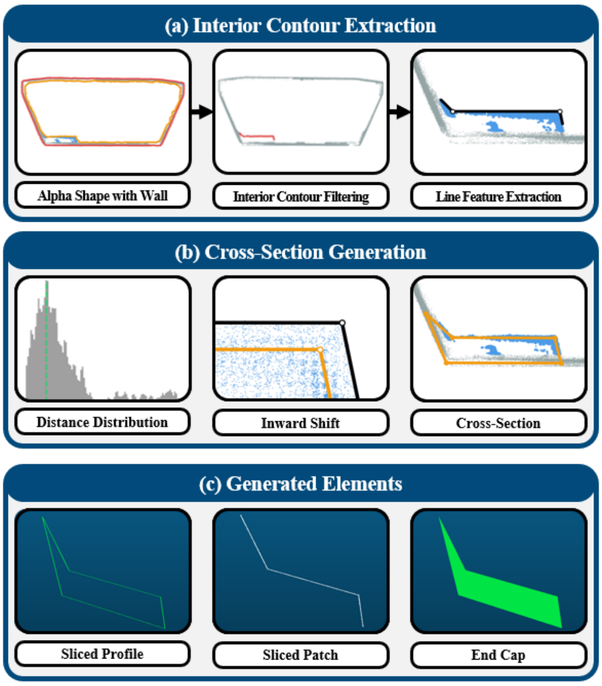

Figure 3. Generation of the three elements used in this study; (a) extraction of the interior contour, (b) cross-section generation, and (c) generated elements.

component is generated and traverses across the target region within the point cloud data. If the distance between points in the patch and the target point cloud data falls below a predefined threshold, the presence of the component is confirmed. This algorithm was originally proposed for detecting standardized components within scaffolding structures. In this paper, the algorithm was modified to a sliced patch-based approach.

Figure 3 illustrates the generation of patch elements used in the proposed algorithm, consisting of interior contour extraction, cross-section generation, and element generation. In Figure 3(a), the segmented point cloud of each component is projected onto the YZ plane and individual instances are separated using DBSCAN-based clustering. The wall point cloud is also projected, and the alpha shape algorithm is applied to the combined point cloud of the component and wall to extract the outer contour. Boundary edges for which either endpoint belongs to the wall point cloud are then removed, retaining only the edges corresponding to the interior surfaces. RANSAC-based line feature extraction [11] is applied to the remaining edges to extract parametric line segments Figure 3(b) shows the cross-section generation step, in which the distances from all points to the extracted contour are computed, and the line segments are inwardly offset to μ to align them with the actual surface location. The outermost line segments are then extended to the wall polygon to form a closed polygonal cross-section. Figure 3(c) shows the three elements generated from the refined cross-section: the sliced profile, created by extruding the contour with a thickness of 1 cm in the X-axis direction; the sliced patch, generated by sampling 4,000 points from the interior surface; and the end cap, generated by filling the interior of the contour with a mesh.

Figure 4 illustrates the procedure for generating 3D CAD models of components using the proposed algorithm. As shown in Figure 4(a), the segmented point cloud data of each class is projected onto the YZ plane along with its corresponding sliced patch to obtain a 2D point cloud data. For components arranged in two rows, such as the deviator block and top temporary PT bar anchor block, the left and right sides are separated using DBSCAN-based clustering (Figure 4(b)). Figures 4(c), (d), and (e) show the generated sliced patch for each component. The sliced patch is slid along the X-axis in increments of 1 cm, corresponding to the thickness of the sliced profile (Figure 4(f)). The sliding range is defined as the X-axis extent of the clustered segment with a 1 m padding on each side. At each position, the number of points $C(\tau)$ within a threshold distance τ between the sliced patch and the segmented point cloud data is calculated. $C(\tau)$ is defined by the following function:

$$C(\tau) = \sum_{i=1}^{N} 1[d(a_i, B) \leq \tau] \tag{1}$$

Where N is the number of points in the sliced patch, a_i is the i-th point in the sliced patch, B is the segmented point cloud, $d(a_i, B)$ is the distance from a_i to the nearest point in B, and $1[\cdot]$ is an indicator function that returns 1

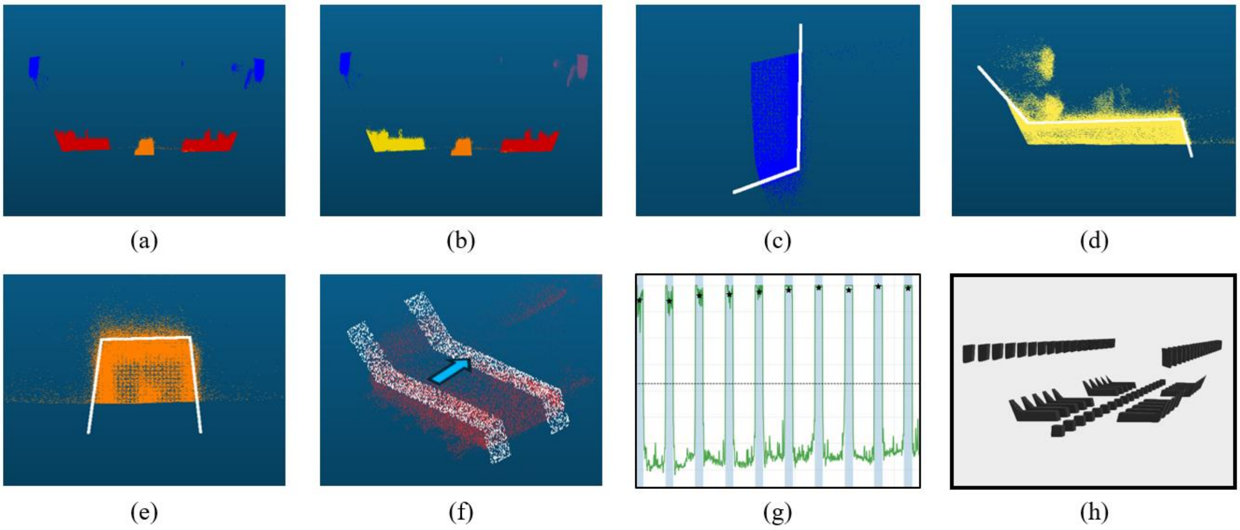

Figure 4. Sliced patch-based 3D reconstruction algorithm; (a) projection of the segmented point cloud onto the YZ plane, (b) left–right separation of the deviator block and top temporary PT bar anchor block using DBSCAN clustering, (c) generated sliced patch of the left top temporary PT bar anchor block, (d) generated sliced patch of the right deviator block, (e) generated sliced patch of the bottom temporary PT bar anchor block, (f) sliding of the sliced patch along the longitudinal direction, (g) binarization of the position– $\boldsymbol{C(\tau)}$ graph using Otsu's algorithm, and (h) 3D reconstruction of individual components.

if the condition is satisfied and 0 otherwise. In this paper, τ was set to 4 cm.

This yields a position– $C(\tau)$ graph along the X-axis. As shown in Figure 4(g), the graph exhibits high point counts when the sliced patch passes through regions where actual components are present. To separate regions where components are present from those where they are absent, the graph is binarized using Otsu's algorithm. Sliced profiles are placed at positions along the sliding axis identified as containing components. Since components composed only of sliced profiles form an open shape at both ends, end caps are added to complete a closed solid geometry. Figure 4(h) shows the 3D reconstruction results of individual components. This algorithm is applied to the deviator block, top temporary PT bar anchor block, and bottom temporary PT bar anchor block. The final combined model is saved as a 3D CAD file.

3 Experiments and Results

3.1 Datasets

To validate the proposed method, interior point cloud data were acquired from three concrete box-girders. A total of 10 interior sections were scanned: 8 from Girders A and B, which contain 18 deviator blocks each, and 2 from Girder C, which contains 20 deviator blocks. In Girder A, deviator blocks are distributed with 10 on the east side and 8 on the west side relative to the cross-sectional center, while Girder B has the opposite distribution with 8 on the east and 10 on the west. Girder C has 10 deviator blocks on each side, totaling 20.

The acquired point cloud data underwent reprocessing. For each dataset, roll and pitch correction was performed, the longitudinal direction of the girder was aligned parallel to the X-axis, and wall points were removed. For datasets with complete boundary contours, wall removal was performed using the proposed wall extraction algorithm — specifically, two datasets from Girder A and one from Girder C. For the remaining datasets, wall removal was performed manually. All other preprocessing steps were performed manually.

For training SuperPoint Transformer, the 10 datasets were split into training, validation, and test sets. The training set consists of 6 datasets: 5 from Girder A and 1 from Girder B. The validation set includes 1 dataset from Girder A and 1 from Girder B. The test set consists of 2 datasets from Girder C, which has a different geometry, to evaluate generalization performance on girders with a different number of deviator blocks. Each point cloud data was manually labeled with the five classes.

Model training was conducted on a workstation running Ubuntu 20.04, equipped with an NVIDIA GeForce RTX 3090 GPU and an Intel Xeon Gold 6240M CPU. The parameters for SuperPoint Transformer were set as follows: voxel size of 1.5 cm, tiling of 2, and batch size of 2. Regularization strength values were set to (0.1, 0.2, 0.3). The maximum number of training epochs was set to 600.

3.2 Experimental Results

3.2.1 3D Semantic Segmentation Results

Table 1 presents the 3D semantic segmentation results. The evaluation metrics used are Intersection over Union (IoU), precision, recall, and F1 score, defined as follows. Here, TP, FP, and FN denote the number of true positive, false positive, and false negative points, respectively.

$$IoU = TP/(TP + FP + FN) \quad (2)$$

$$Precision = TP/(TP + FP) \quad (3)$$

$$Recall = TP/(TP + FN) \quad (4)$$

$$F1\ score = \frac{2(Precision \cdot Recall)}{Precision + Recall} \quad (5)$$

The segmentation achieved a mean IoU (mIoU) of 94.1% and a mean F1 score of 96.9%. Figure 5 shows the segmented test data.

Table 1. Segmentation performance for concrete box-girder interior point cloud data.

Class	IoU	Precision	Recall	F1 score
Deviator block	82.5%	84.2%	97.6%	90.4%
Tendon	97.9%	99.8%	98.1%	98.9%
Top temporary PT bar anchor block	92.7%	92.7%	100.0%	96.2%
Bottom temporary PT bar anchor block	98.5%	99.2%	99.3%	99.2%
Cable tray	98.9%	99.0%	99.9%	99.5%
Average	94.1%	95.0%	99.0%	96.9%

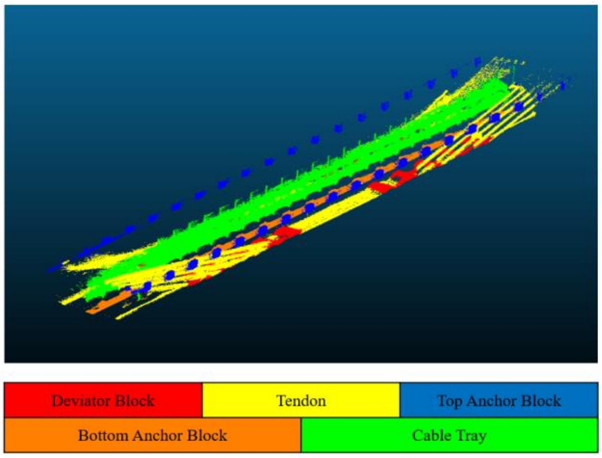

Figure 5. Segmentation result.

3.2.2 3D CAD Model Generation Result

Sliced profiles, sliced patches, and end caps for each component were generated from the segmented point cloud and applied to the 3D reconstruction. Table 2 presents the mean mesh-to-point cloud distance. For each point in the segmented point cloud, the distance to the nearest polygon of the generated mesh was calculated. The proposed method achieved mean distances of 0.025 m against the point cloud data. Figure 6 shows the 3D CAD model generation results.

Table 2. Mean mesh-to-point distance results for the generated 3D CAD models compared with the point cloud.

Class	Mesh-to-point cloud distance
Wall	0.007 m
Deviator block	0.002 m
Top temporary PT bar anchor block	0.080 m
Bottom temporary PT bar anchor block	0.010 m
Average	0.025 m

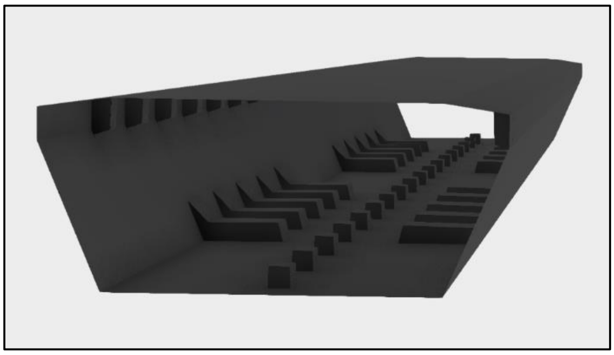

Figure 6. Generated 3D CAD model of the concrete box-girder interior.

4 Discussion

4.1 Point Cloud Segmentation

The point cloud segmentation results showed that the Top temporary PT bar anchor block, Bottom temporary PT bar anchor block, and Cable tray achieved high IoU values of 92.7%, 98.5%, and 98.9%, respectively.

These classes have minimal physical connections with other components in the concrete box-girder interior point cloud after wall removal, resulting in clear boundaries between classes. This is considered to have contributed to stable segmentation performance. Furthermore, the model demonstrated high performance on test data with a different deviator block arrangement compared to the training data, indicating potential for generalization.

In contrast, the deviator block showed relatively lower IoU values of 82.5%. As shown in Figure 7(a), tendons in contact with deviator blocks were found to be misclassified as deviator blocks. Since tendons structurally pass through deviator blocks and are physically in contact with them, tendon points were misclassified as deviator blocks. Additionally, Figure 7(b) shows cases where tendons were misclassified as cable tray. This is attributed to the tendons extending upward and approaching the locations where the cable tray is present.

4.2 3D CAD model generation

The proposed sliced patch-based 3D reconstruction algorithm achieved mean mesh-to-point cloud distances of 0.025 m against the point cloud and successfully generated 3D CAD models by separating components at the instance level from semantically segmented point cloud data. Notably, the proposed method reconstructed 3D CAD models using only the point cloud data.

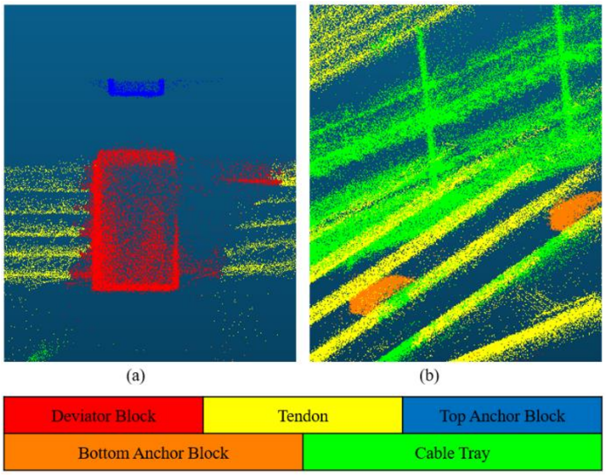

Figure 7. Examples of misclassification in point cloud segmentation results; (a) tendon misclassified as a deviator block, and (b) tendons misclassified as a cable tray.

However, cases were observed where the generated 3D CAD models differed from the actual geometry. Figure 8(a) shows a case where multiple 3D CAD models were generated for a single component. This occurred due to variability in the position– $C(\tau)$ graph constructed from nearest-neighbor relationships between the patch and point cloud, causing the Otsu-based binarization to segment a single continuous component into multiple fragments. Figure 8(c) shows a case where a 3D CAD model was generated for only a partial region of a component rather than the entire geometry. This is attributed to sparse points on all surfaces of the segment during scanning, resulting in missing points in certain regions.

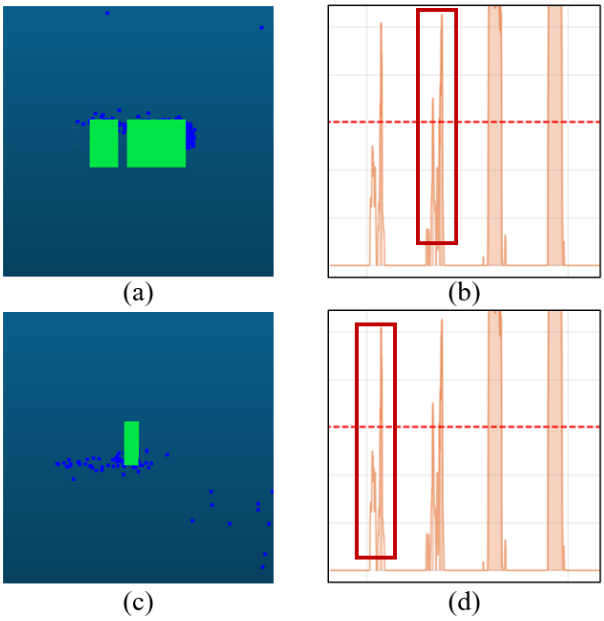

Figure 8. Examples of incorrect 3D reconstruction; (a) a top anchor block fragmented into two parts, (b) a segment split by Otsu algorithm-based binarization (highlighted by the red box), (c) a model generated only on the right-side surface, and (d) an excessively thin segment remaining after Otsu algorithm-based binarization (highlighted by the red box).

4.3 Future Development

This paper presented a procedure for segmenting concrete box-girder interior point cloud data using SuperPoint Transformer and reconstructing 3D CAD models from the segmented results. The proposed framework was applied to actual bridge girder data, demonstrating its potential applicability to concrete box-girder inspection by performing semantic segmentation and 3D reconstruction on girder data with different interior environments. However, several aspects require further improvement.

First, the proposed framework does not include a 3D reconstruction methodology for tendons. Considering the significance of a tendon in a concrete box-girder, it is necessary to develop a parametrization method for tendons and integrate it into the proposed framework.

Second, the validation of the proposed methodology was limited to data acquired from a single bridge. Therefore, it is necessary to verify the generalization performance on bridges with different internal structures. Additional concrete box-girder interior data from multiple bridges with varying interior geometries, component configurations, and scan qualities should be acquired, and performance should be validated by applying the same pipeline to enhance practical applicability.

Third, several steps in the proposed pipeline were performed manually. Roll and pitch correction and axis alignment, and diaphragm removal were conducted manually, and the parameters for SOR-based noise removal, the alpha shape algorithm, and RANSAC based line extraction were heuristically determined. Automating these procedures is necessary.

Fourth, the proposed sliced patch-based algorithm is applicable only to components that are linear and have a constant cross-sectional profile along their length. For components with varying cross-sections or curved geometries, alternative reconstruction approaches would be required.

5 Conclusion

This paper presents a framework for semantic segmentation of point cloud data acquired from the interior of a concrete box-girder and 3D CAD model reconstruction of individual components. The proposed methodology was validated on actual concrete box-girder data, achieving a semantic segmentation performance of 94.1% mIoU. The mean mesh-to-point cloud distance was 0.025 m against the point cloud data, demonstrating the feasibility of the proposed approach. By addressing the identified limitations and refining the methodology in future work, this paper is expected to contribute to the establishment of 3D data-driven inspection systems for interiors of a concrete box-girder.

Acknowledgment

This work was supported by the National Research Foundation of Korea (NRF) grant funded by the Ministry of Education (No. RS-2018-NR031077). This work was supported by the National Research Foundation of Korea (NRF) grant funded by the Korea government (MSIT) (RS-2024-00457308). ※ MSIT: Ministry of Science and ICT. This research was conducted with the support of i-thetto Co., Ltd. and Korea Expressway Corporation.

References

[1] Seoul Metropolitan Government. Announcement of defect causes and PSM bridge inspection results for Jeongneungcheon Overpass On-line: https://news.seoul.go.kr/safe/archives/46885, Accessed: 14/01/2026.

[2] Seoul Facilities Corporation. Damage Investigation and Repair Progress of Cheongdam 1st Bridge. On-line: https://www.sisul.or.kr/open_content/main/introduce/innovation5.jsp, Accessed: 14/01/2026.

[3] Fang Y., Mitoulis S.-A., Boddice D., Yu J., and Ninic J. Scan-to-BIM-to-Sim: Automated reconstruction of digital and simulation models from point clouds with applications on bridges. *Results in Engineering*, 25:104289, 2025.

[4] Jing Y., Sheil B., and Acikgoz S. Segmentation of large-scale masonry arch bridge point clouds with a synthetic simulator and the BridgeNet neural network. *Automation in Construction*, 142:104459, 2022.

[5] Kim Y., Kim J., Kim J., and Kim H. Superpoint Transformer-Based Bridge Component Recognition Using UAV-Mounted LiDAR and Synthetic Point Cloud Generation. *Journal of Computing in Civil Engineering*, 39(4):04025043, 2025.

[6] Yang L., Lin Y.-C., Cai H., and Habib A. From Scans to Parametric BIM: An Enhanced Framework Using Synthetic Data Augmentation and Parametric Modeling for Highway Bridges. *Journal of Computing in Civil Engineering*, 38(3):04024008, 2024.

[7] Shu J., Zeng Z., Li W., Zhou S., Zhang C., Xu C., and Zhang H. Automatic geometric digital twin of box-girder bridge using a laser-scanned point cloud. *Automation in Construction*, 168(A):105781, 2024.

[8] Zhu Y., Diaw I., and Xiong W. Cable-stayed bridge all-round morphology identification based on 3D point cloud model. *Structure and Infrastructure Engineering*, 22(2):185–200, 2026.

[9] Xu W., Cai Y., He D., Lin J., and Zhang F. FAST-LIO2: Fast Direct LiDAR-inertial Odometry. On-line: https://arxiv.org/abs/2107.06829, Accessed: 14/01/2026.

[10] Wang Y. FAST_LIO_LC: The tight integration of FAST-LIO with Radius-Search-based loop closure module. On-line: https://github.com/yanliang-wang/FAST_LIO_LC, Accessed: 13/01/2026.

[11] Mahmoud M., Chen W., Yang Y., and Li Y. Automated BIM generation for large-scale indoor complex environments based on deep learning. *Automation in Construction*, 162:105376, 2024.

[12] Robert D., Raguet H., and Landrieu L. Efficient 3D Semantic Segmentation with Superpoint Transformer. On-line: https://arxiv.org/abs/2306.08045, Accessed: 13/01/2026.

[13] ASBI-Assoc. Design Manual for Concrete Segmental Bridges, 1st Edition. On-line: https://asbi-assoc.org/wp-content/uploads/2025/10/ASBI-Design-Manual-for-Concrete-Segmental-Bridges-1st-Edition-2.pdf, Accessed: 13/01/2026.

[14] Kim J., Kim J., Kim Y., and Kim H. 3D reconstruction of large-scale scaffolds with synthetic data generation and an upsampling adversarial network. *Automation in Construction*, 156:105108, 2023.